



## Review

## Spin-crossover phenomena in extended multi-component metallo-supramolecular assemblies

Y. Bodenthin<sup>a,b</sup>, G. Schwarz<sup>c,d</sup>, Z. Tomkowicz<sup>e,g</sup>, M. Lommel<sup>a</sup>, Th. Geue<sup>f</sup>, W. Haase<sup>g</sup>,  
H. Möhwald<sup>c</sup>, U. Pietsch<sup>a</sup>, D.G. Kurth<sup>c,d,h,\*</sup>

<sup>a</sup> University Siegen, FB7 Solid State Physics, D-57068 Siegen, Germany

<sup>b</sup> Swiss Light Source, Paul Scherrer Institut, CH-5232 Villigen-PSI, Switzerland

<sup>c</sup> Max Planck Institute of Colloids and Interfaces, D-14424 Potsdam, Germany

<sup>d</sup> Chemische Technologie der Materialsynthese, Julius-Maximilians-Universität Würzburg, Röntgenring 11, D-97070 Würzburg, Germany

<sup>e</sup> Institute of Physics, Jagellonian University, Reymonta 4, 30-059 Kraków, Poland

<sup>f</sup> Laboratory for Neutron Scattering, ETH Zurich and Paul Scherrer Institut, CH-5232 Villigen, Switzerland

<sup>g</sup> Institute of Physical Chemistry, Darmstadt University of Technology, Petersenstrasse 20, D-64287 Darmstadt, Germany

<sup>h</sup> National Institute for Materials Science, 1-1 Namiki, Tsukuba, Ibaraki 305-0044, Japan

## Contents

1. Introduction.....	2415
2. Basic concepts .....	2415
2.1. Main concept of structure-induced spin-crossover .....	2415
2.2. Liquid crystals and spin-crossover .....	2416
2.3. Examples of spin-crossover induced by structure phase transitions.....	2416
2.4. Metallo-supramolecular grid nanostructures .....	2417
2.5. Control of spin-crossover by ligand design in 2,2':6',2''-terpyridines .....	2417
3. Metallo-supramolecular polyelectrolyte-amphiphile complexes.....	2417
4. Thin films .....	2418
4.1. Magnetic and structural properties of thin metallo-supramolecular films.....	2418
4.2. Other examples of spin-crossover in thin films .....	2419
5. Volume material .....	2419
5.1. Structural and magnetic properties of bulk PAC .....	2419
6. Rigid metallo-polymers and alternative ligand concepts .....	2420
7. Outlook and perspectives .....	2421
Acknowledgements.....	2421
References .....	2421

## ARTICLE INFO

## Article history:

Received 1 August 2008

Accepted 20 October 2008

Available online 6 November 2008

## Keywords:

Supramolecular chemistry  
Metallo-supramolecular coordination  
polymers  
Liquid crystals  
Self-assembly  
Molecular magnetism

## ABSTRACT

The combination of liquid crystals and spin-crossover (SCO) in one compound offers exciting perspectives for magnetic materials. The liquid crystalline organization of SCO compounds adds another dimension to magnetic materials. The SCO compounds can be for instance reoriented through external fields, which alters the optical properties. In addition, the LC phase transition can induce a SCO in the embedded compounds by inducing mechanical strain, which can perturb the coordination geometry of the central metal ions thus giving rise to a change in the electronic and magnetic properties. So far, this concept has only been implemented in a few material combinations. Here, we review the magnetic properties in metallo-supramolecular coordination polyelectrolyte-amphiphile complexes (PACs).

© 2008 Elsevier B.V. All rights reserved.

\* Corresponding author at: Julius-Maximilians-University Würzburg, Chemische Technologie der Materialsynthese, Röntgenring 11, D-97070 Würzburg, Germany.  
E-mail addresses: [yves.bodenthin@psi.ch](mailto:yves.bodenthin@psi.ch) (Y. Bodenthin), [dirk.kurth@matsyn.uni-wuerzburg.de](mailto:dirk.kurth@matsyn.uni-wuerzburg.de) (D.G. Kurth).

## 1. Introduction

In the recent years there has been great interest in the study of the magnetic properties of molecular compounds [1,2]. As a result, the research field of molecular magnetism represents a very lively scientific area where both physicists and chemists join their efforts to design molecular architectures containing magnetic metal centers with novel magnetic properties [3–5]. Many molecular magnetic compounds developed to date offer interesting scientific and technological perspectives for information storage and processing [6], signal transduction [7] or novel quantum mechanical effects at nanometer length scale [8]. The first room-temperature organo-metallic magnets were reported in 1991 [9] and 1995 [10]. In the same period, molecular magnets consisting of pure organic radicals were first published [11]. Also, new types of magnets with unusual properties have been reported, for example, single-molecule magnets and single-chain magnets exhibiting a hysteresis loop in 0- or 1-dimension [12–15]. Recently it has been theoretically shown that in purely isotropic spin systems, e.g. symmetric spin icosahedrons, magnetic switching can be induced despite the absence of structural or magnetic anisotropy effects due to geometrical frustration [16]. In symmetric spin icosahedrons spins are mounted on the vertices of edge sharing triangles and coupled through nearest-neighbor, antiferromagnetic isotropic Heisenberg exchange interactions and switch when an

external magnetic field equals a critical value. Another important contribution to the research field of molecular magnetism was provided by supramolecular chemistry: self-assembly of molecular building blocks like transition metal ions, tailored ligands and amphiphiles allows the development of complex functional supramolecular architectures with unique electronic and magnetic properties in a rational way. A central objective is the structure tuning of these molecular magnetic compounds with (at least) two different stable electronic or magnetic states within a specific temperature range. External perturbations can be used to cause a specific structure variation which is strong enough to affect magnetic properties. For example, thermal spin transition (spin-crossover (SCO)) is one of the most fascinating and most extensively explored dynamic electronic structure phenomena in coordination chemistry. Self-assembly has therefore become a central concept for the preparation of tunable spin-crossover compounds and represents an expanding area of today's chemical research [17–19]. Given its versatility, power, and potentially facile applicability, self-assembly has gained remarkable attention as a viable technique to design complex, metallo-supramolecular architectures based on non-covalent interactions [20]. These materials, build by metal–ligand complexation, are especially intriguing for the implementation of novel structures and magnetic properties.

This article focuses on the properties and magneto-structure correlations of systems composed of transition metal ions and terpyridine (tpy) based or related ligands. At the beginning, we describe the main concept of a structure-induced spin-crossover in polyelectrolyte-amphiphile complex (PAC). Next we highlight some of the neighboring research areas: e.g. spin-crossover in liquid crystals, alternative concepts of structure controlled spin-crossover, tpy-based metallo-supramolecular grid structures or the control of spin-crossover by ligand design. At the end of this article an outlook and perspectives are given.

## 2. Basic concepts

### 2.1. Main concept of structure-induced spin-crossover

The concept of structure-induced spin-crossover was first demonstrated in Langmuir–Blodgett (LB) multilayers of a PAC self-assembled from 1,4-bis(2,2':6',2''-terpyridine-4'-yl)benzene, Fe(II) and the amphiphile dihexadecyl phosphate (DHP) (for a detailed description of the complex please refer to Section 3) [21]. The stoichiometry of metal ions to DHP was 1:6 in this case. The PAC architecture consists of DHP double layers, where the interstitial space is occupied by the rod-like metallo-supramolecular polyelectrolyte (MEPE) [22]. A phase transition in an amphiphilic mesophase is explored to deliberately induce sufficient mechanical strain in the embedded metallo-supramolecular assembly of tightly coupled metal ion coordination centers. Melting of the alkyl chains causes distortion of the coordination geometry around the central metal ion. As a result, the crystal field splitting of the d-orbital subsets decreases resulting in a spin transition from a low-spin (LS) to a high-spin (HS) state. The LB-film shows a reversible, partial spin-crossover slightly above room temperature. The change in the spin state of the transition metal ions causes a transition from diamagnetic to paramagnetic. An overview of the general concept is outlined in Fig. 1.

Later on, the concept of structure-induced spin-crossover was adopted by Hayami et al. to achieve a reverse (HS → LS) spin transition in Fe(II) complexes with terpyridine ligands modified by long alkyl chains [23]. Independently, Ruben et al. recently reported a spin transition in linear Fe(II) terpyridyl-based metallo-polymers (Section 6) [24].

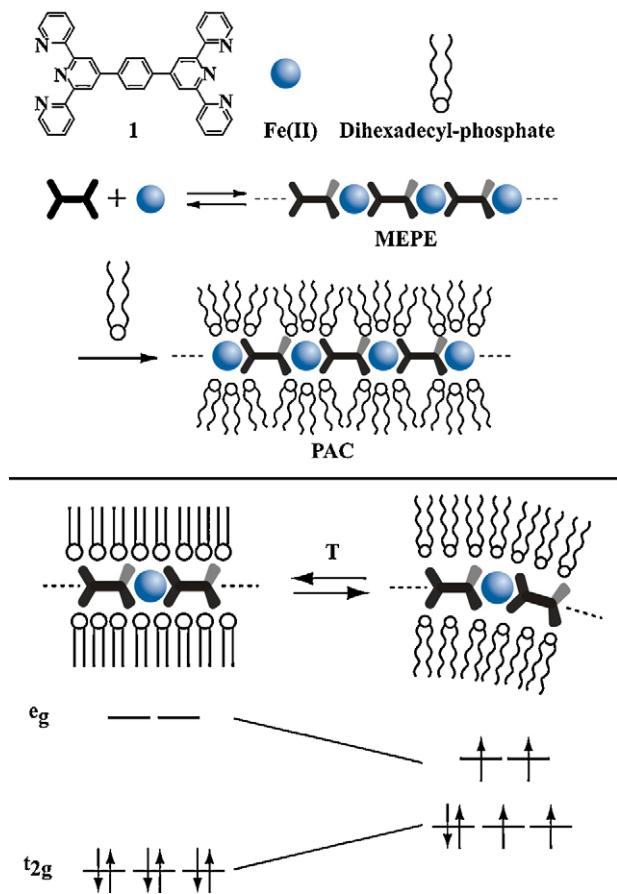


**Fig. 1.** Top: self-assembly of the ditopic bis(terpyridine) ligand and iron acetate in aqueous solution results in the formation of a metallo-supramolecular polyelectrolyte (MEPE). The subsequent self-assembly of MEPE and dihexadecyl phosphate (DHP) affords the polyelectrolyte-amphiphile complex (PAC). Bottom: melting of the alkyl chains in the amphiphilic mesophase induces a spin transition from a diamagnetic LS state (left) to a paramagnetic HS state (right). For simplicity an octahedral symmetry of the metal ion is assumed. Reprinted with permission from Ref. [21].

The extensive control of structure and function provided by self-assembly of molecular building blocks like Fe(II) ions and tpy-based ligands gives access to a wide range of new molecular magnetic architectures such as nanostructures, thin films, and liquid crystals. A brief overview of selected spin transition materials and the mechanisms involved in structure-controlled spin-crossover are given in the following sections.

## 2.2. Liquid crystals and spin-crossover

Liquid crystals (LCs) were discovered more than a century ago and since then gained remarkable interest with the discovery of the twisted nematic effect, which launched the era of liquid crystal applications [25]. The simultaneous occurrence of crystal like order and liquid like mobility in LCs allows the reorientation of polar, rod like molecules through an external electric field, which alters the optical properties of the material. This effect is the foundation of liquid crystal displays technology (LCD). In recent years, the design of metal-containing liquid crystals (metallomesogens) has attracted much attention because of the possibility to align paramagnetic liquid crystals by weak magnetic fields. The particular features of liquid crystalline phases and spin-crossover compounds have stimulated the idea of combining both properties in a single material as for example the design of thin films containing SCO materials.

As a first example for the coexistence of SCO and LC properties, pseudooctahedral Fe(III) complexes with  $N_4O_2$  coordination were investigated, whereby Schiff-base ligands with elongated substituents provided a rod-like geometry and the liquid crystalline properties of the complex [26]. The spin-crossover and the LC phase transitions do not occur in the same temperature region and they are not coupled. In general, one can distinguish three types of synergy between SCO and LC phase transitions in metallomesogens. First, systems where both phase transitions are interrelated and occur at the same temperature, second, systems where both transitions are not interrelated but inadvertently occur in the same temperature region and, third, systems with independent phase transitions at different temperatures [27]. This classification was derived from investigations of Fe(II) metallomesogens based on the ligand tris[3-aza-4-((5- $C_n$ )(6-R)(2-pyridyl))but-3-enyl]amine. Depending on the alkyl chain length ( $C_n$  with  $n = 6, 12, 16, 18$  and 20) and R = hydrogen or methyl ( $C_{6,16,18,20}$ -trenH or  $C_{6,12,18}$ -trenMe) the complexes belong to one of the above mentioned types.

A first example where the LC phase transition in an amphiphilic matrix induces a SCO is realized in metallo-supramolecular PACs. In these systems, the spin-state transition is induced by the mechanical strain associated with the LC phase transition of an amphiphilic mesophase, which embeds the otherwise magnetically inactive metallo-supramolecular coordination polyelectrolyte as described in the following.

## 2.3. Examples of spin-crossover induced by structure phase transitions

Hayami et al. described a way to control the spin-crossover in tpy-based transition metal ion complexes with covalently bonded alkyl chains whereby the spin transition temperature depends on the alkyl chain length [23]. The Co(II) complex  $[Co(C_{16}\text{-tpy})_2](BF_4)_2$  ( $C_{16}\text{-tpy} = 4'$ -hexadecyloxy-2,2':6',2''-terpyridine) shows a reverse ( $HS \rightarrow LS$ ) spin transition with large thermal hysteresis. Thereby, the Co(II) ion changes between  $S = 3/2$  and  $S = 1/2$  spin states. Usually, the HS state emerges in the high temperature phase and the LS state is usually observed in the low temperature phase. In this case, the opposite transition is observed, that is the LS-to-HS transition is induced by cooling and the reverse transition is induced by warming. The spin-crossover is thermally induced just below room

temperature with a hysteresis width of 43 K.  $[Co(C_{14}\text{-tpy})_2](BF_4)_2$  ( $C_{14}\text{-tpy} = 4'$ -tetradecyloxy-2,2':6',2''-terpyridine) also exhibited a reverse spin transition at room temperature with a very large hysteresis width ( $\Delta T = 56$  K). The authors postulated, supported by XRD measurements, that the reverse spin transition is induced by a structural phase transition, e.g. through packing effects in the solid state through strong intermolecular forces. However, the melting of the alkyl chains occurs approximately 100 K above the SCO temperature and is, therefore, considered an independent LC phase transition.

Later on, Hayami et al. reported a simultaneous SCO–LC phase transition around room temperature in the compound  $[Co(C_5C_{12}C_{10}\text{-tpy})_2](BF_4)_2$  [ $C_5C_{12}C_{10}\text{-tpy} = 4',5'''$ -decyl-1'''-(heptadecyloxy)-2,2':6',2''-terpyridine] (Fig. 2) [28]. The employed ligand is based on a terpyridine frame with attached branched alkyl chains providing a pseudo-octahedral environment of the coordinated Co(II) ion. The spin-crossover and liquid crystalline phase transition were investigated by measurements of the molar magnetic susceptibility  $\chi_m$ , powder X-ray diffraction, and differential scanning calorimetry. An abruptly increasing susceptibility at around  $\sim 88$  K signals the spin-crossover from the LS to the HS state. The spin transition is directly related to a mesophase transition found by X-ray diffraction. On cooling, the magnetic susceptibility decreased abruptly at around  $\sim 284$  K, showing that the HS moieties were restored to the LS state with a small hysteresis loop ( $\Delta T \sim 4$  K). Additional thermal cycles did not alter the thermal hysteresis loop. Below the phase transition, the branched alkyl chains do not melt, and the Co–N bond distance in the LS state is short. Upon heating, the branched alkyl chains melt and the spin transition from the LS to HS states occurs permitting elongation of the Co–N bonds.

Another example of a spin transition triggered by a phase transition in a Fe(II) based metallo-supramolecular complex has been reported by Fujigaya et al. [29]. A rigid coordination polymer was made from triazole ligands with two long alkyl chains ( $C_n\text{trz}$ ) bridging the iron(II) centers. In the solid-state, polynuclear species are formed by interdigitation of the long alkyl chains. At low temperatures, the crystalline alkyl chains of ( $C_n\text{trz}$ )Fe(II), upon interdigitation, most likely lock the Fe–N bond distance of the low-

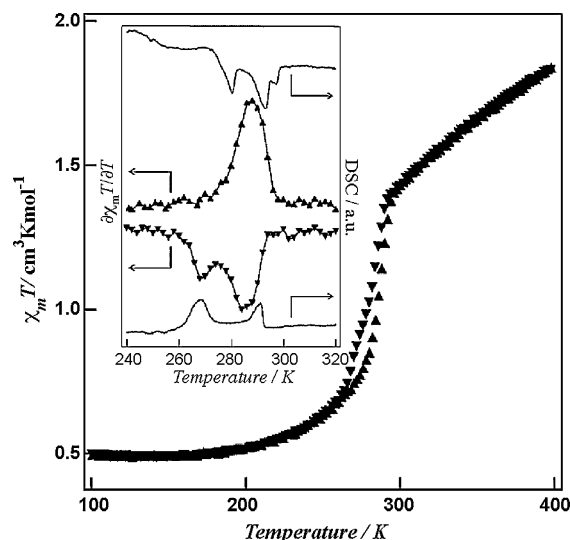


**Fig. 2.**  $\chi_m T$  vs.  $T$  plot (standing triangles, heating mode; hanging triangles, cooling mode) for  $[Co(C_5C_{12}C_{10}\text{-tpy})_2](BF_4)_2$ ; a Co(II) complex based on a terpyridine frame with attached branched alkyl chains. The inset graph shows the derivative  $\delta\chi_m T/\delta T$  plot and the corresponding DSC curve as a function of temperature. Reprinted with permission from Ref. [28].

spin Fe(II) complex. On heating, the lock can be released by melting of the alkyl chains, thereby permitting elongation of the Fe–N bond, necessary for the transition to the HS state.

#### 2.4. Metallo-supramolecular grid nanostructures

In the last decade, it was realized that the interplay between spin-crossover and magnetic coupling could be exploited to govern the magnetic properties of molecular compounds. It was expected that the intramolecular ferromagnetic or antiferromagnetic coupling could be suppressed or enhanced alternating the spin state of the metal centers. Extension of this approach to 2D and 3D supramolecular assemblies would enable one to combine two phenomena in the same solid, namely magnetic ordering and spin-crossover. The goal is to investigate how the magnetic ordering can influence the spin-crossover process. The development of molecular clusters in which more than one metal ion is incorporated is therefore an interesting subject. A particularly interesting class of compounds is that of the supramolecular  $[N \times N]$  grid structures (Fig. 3) [30]. In these complexes, the ligand includes two tpy-units. The assembly of four ligands with four transition metal ions results in an essentially flat, square, grid-like arrangement of metal ions realizing a pseudo-octahedral coordination environment for each ion. The strength of the ligand field can be variably adjusted by either steric strain or steric repulsion. From the magnetic perspective, the grids may be regarded as molecular model systems for magnets with extended magnetic interactions like intramolecular antiferromagnetic coupling. Numerous grids containing the transition metal ions Cu(II), Co(II), Mn(II), Ni(II) have been created, and studies have shown a remarkable variety of their magnetic properties [31–34]. In the context of spin-crossover, the tetranuclear Fe(II) complex  $[\text{Fe}_4\text{L}_4](\text{ClO}_4)_8$  ( $\text{L} = 4,6\text{-bis}(2',2''\text{-bipyridine-6'-yl})\text{-2-phenylpyrimidine}$ ) is most intriguing [35]. It presents a threefold switchable system, which shows three successive spin transitions of the form  $\text{HS-HS-HS-LS} \leftrightarrow \text{HS-HS-LS-LS} \leftrightarrow \text{HS-LS-LS-LS}$ . These transitions could be induced by changing temperature or by application of pressure. Switching the spin state from LS to HS by light

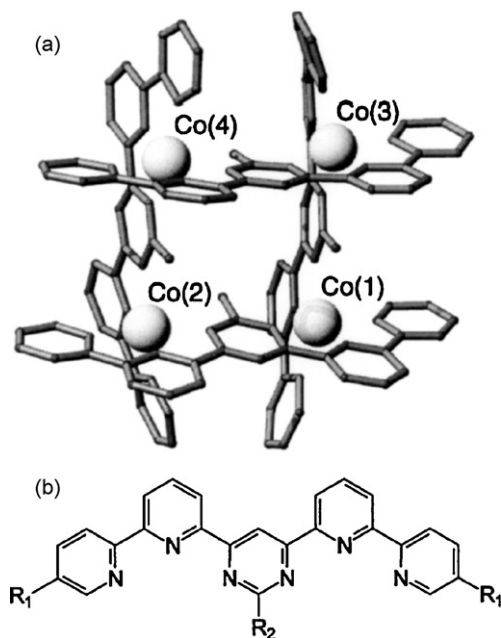


**Fig. 3.** (a) Representative example of a supramolecular  $[N \times N]$  grid structure with Co(II) as metal ion. (b) Bis(bipyridyl)-pyrimidine ligand with  $\text{R}_1 = \text{H}$  and  $\text{R}_2 = \text{CH}_3$ . Figure reprinted from Ref. [32].

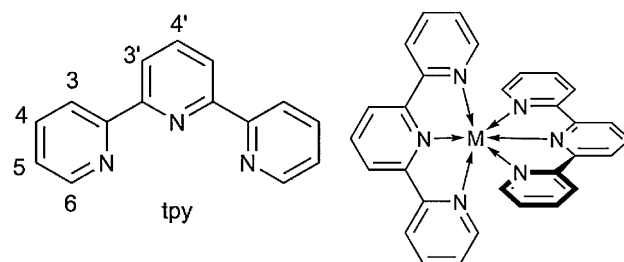


**Fig. 4.** Left: the numbering scheme for substituents in 2,2':6',2''-terpyridines. The nitrogen atoms are arranged in the *cis,cis* conformation to form this  $\text{M}(\text{tpy})_2$  motif. Right: the idealized  $\text{D}_{2d}$  structure of a  $\text{M}(\text{tpy})_2$  motif. Reprinted from Ref. [43].

(LIESST effect) [36] is possible with green light at 514 nm and temperatures below 5 K. Recorded Mössbauer spectra of the Fe(II) grid at different temperatures and permanent irradiation with green light revealed a light-induced thermal hysteresis (LITH) [37]. This implies the presence of intramolecular cooperativity between the Fe(II) metal centers.

#### 2.5. Control of spin-crossover by ligand design in 2,2':6',2''-terpyridines

As mentioned in the last section, the spin-crossover of metallo-supramolecular complexes can be controlled by design of the tpy-based ligands. In the following, different examples are given in order to achieve designated spin states of the central metal ion by different substituents on different positions at the tpy-ligand. 2,2':6',2''-terpyridines without any substituents form low-spin  $[\text{Fe}(\text{tpy})_2]\text{X}_2$  complexes irrespective of the counterion X [38]. The appropriate numbering of 2,2':6',2''-terpyridine ligands is presented in Fig. 4. The introduction of substituents at the 4'-position has no effect on the spin state [39]. Minor effects on the spin state were observed for substituents in the 5,5'' position. In particular, the investigated Fe–N distances in  $\text{Fe}(\text{tpy})_2$  complexes with electron releasing and electron withdrawing groups (5,5''-dinitro, 5,5''-alkoxy) shows the central metal ion to be situated in the low-spin state [40].

In order to modify 2,2':6',2''-terpyridine ligands to be capable to form spin-crossover complexes the introduction of steric strain or steric bulk close to the donor atoms is possible. The introduction of phenyl substituents at both the 6- and 6''-positions leads exclusively to the formation of orange high-spin Fe(II) complexes whilst the presence of a single 6-phenyl substituent results in spin-crossover systems [41]. An interesting exception from this picture demonstrates the substitution of 2,2':6',2''-terpyridines with phenyl groups at the 4,4'' position. In this case, the coordination geometry is highly distorted and lies between a highly distorted sixfold coordinated complex and a fourfold coordinated compound with two additional weak interactions. The phenyl rings are  $\pi$ -stacked (approximately coplanar, interplanar distances 3.2–3.6 Å) with one central and one terminal ring of the other ligand [41].

#### 3. Metallo-supramolecular polyelectrolyte-amphiphile complexes

In this section we are going to introduce in more detail the metallo-supramolecular amphiphile complex (PAC) already mentioned above. The self-organization of PAC is schematically shown in Fig. 1. Metal ion induced self-assembly of the ditopic terpyridine ligand 1,4-bis(2,2':6',2''-terpyridine-4'-yl)benzene **1** with  $\text{Fe}(\text{OAc})_2$  results in formation of the blue colored Fe(II) metallo-supramolecular polyelectrolyte (MEPE) [42]. With Fe(II)



ions terpyridine (tpy) forms stereochemically defined pseudo-octahedral complexes with  $D_{2d}$  symmetry [43]. Treating an aqueous solution of MEPE with a chloroform solution containing dihexadecylphosphate (DHP) results in instant transfer of Fe(II)-PAC into the organic phase [44]. After drying and evaporating the organic phase, PAC is isolated as dark blue powder, which is soluble in common organic solvents. The formation of PAC is confirmed by UV-vis, NMR, and IR spectroscopy. The IR and NMR spectra show that the acetate counter ions of MEPE qualitatively are replaced by amphiphiles. The stoichiometry between the amphiphiles and the metallo-supramolecular repeat unit (and therewith Fe(II) ion) is readily adjusted through the self-assembly conditions.

#### 4. Thin films

##### 4.1. Magnetic and structural properties of thin metallo-supramolecular films

The metallo-supramolecular PACs form a stable monolayer at the air–water interface that are readily transferred and oriented on a solid support [44]. The measured  $\pi$ -A isotherm was found to be reproducible with a slight hysteresis. It shows no distinct phase transitions and a remarkably high collapse pressure ( $>60$  mN/m). The PAC rearranges such that the amphiphiles form a compact monolayer located at the top, whereas the Fe(II)-MEPE is in contact with the water interface. It is assumed that this composite structure enhances the stability of the Langmuir monolayer. The monolayer can be transferred onto solid supports by means of the Langmuir–Blodgett technique resulting in thin anisotropic films of PAC [22].

A detailed structure analysis of a LB multilayer was performed by X-ray reflectometry (XRR), extended X-ray absorption fine structure measurements (EXAFS) and temperature dependent energy-dispersive X-ray scattering [22,45]. Fig. 5 shows the measured and the calculated X-ray reflectivity as a function of the vertical momentum transfer  $q_z$ . The inset in Fig. 5 shows the calculated electron density profile, which is used to fit the reflectivity data. The obtained electron density profile matches the proposed structure of PAC (see Fig. 1). The multilayer has a periodicity of 57 Å, which corresponds to an architecture of upright-standing closely packed amphiphilic layers embedding the metallo-supramolecular

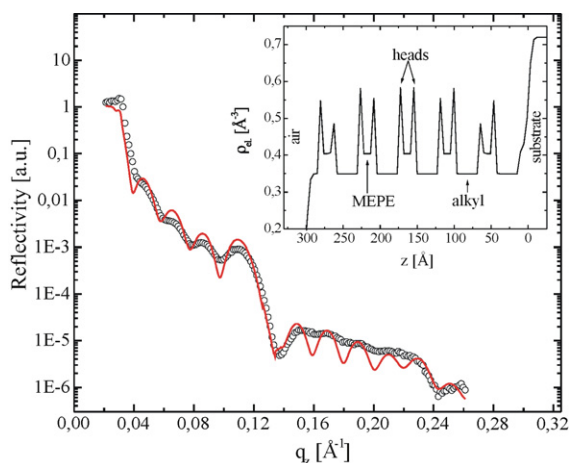


**Fig. 5.** Experimentally determined and calculated reflectivity vs.  $q_z$  of a LB film consisting of 11 PAC monolayers. The Bragg peaks correspond to a periodicity of 57 Å and the Kiessig fringes to a total film thickness of 311 Å, respectively. The inset shows the resulting electron density profile. The zero-position marks the film–air interface. Figure according Ref. [22].

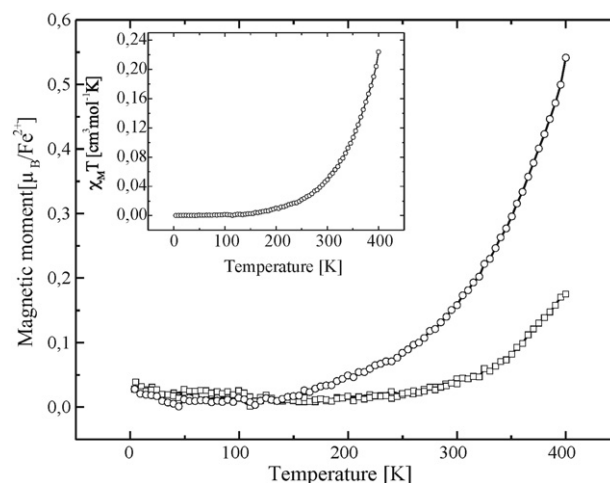


**Fig. 6.** Temperature dependent magnetic moments for two PAC LB films consisting of 11 and 15 layers. The material is diamagnetic at low temperatures and becomes paramagnetic above room temperature. Inset: measurement of the molar susceptibility as  $\chi_m T$  vs.  $T$ . Figure reprinted with permission from Ref. [21].

coordination polyelectrolyte (MEPE) rods. The total film thickness is found to be  $\sim 311$  Å.

The in-plane structure of the film was investigated by grazing incidence diffraction (GID). At this technique the incident X-ray beam strikes the sample surface at a grazing angle of  $\alpha_i \sim 0.2^\circ$ . The beam is diffracted at the in-plane lattice planes created by the lateral arrangement of DHP molecules. The diffraction pattern corresponds to a hexagonal arrangement with a lattice spacing of  $d_{\text{in}} = 4.2$  Å, which is in agreement with values found in PAC films at the air–water interface [46] and in other LB-films e.g. of fatty acid salts [47]. Temperature induced changes in structure of these films were investigated simultaneously by energy-dispersive X-ray reflectivity and in-plane diffraction. The multilayer shows a reversible phase transition in the temperature range from room temperature up to 328 K. With increasing temperature the lateral ordering of the alkyl chains is lost and the vertical layering and smoothening of the multilayer is reduced upon heating. Cooling restores the initial film structure. Using extended X-ray absorption fine structure (EXAFS) experiments at the iron K-absorption edge the next-neighbor coordination geometry around the central Fe(II) ions was determined to be pseudo-octahedral. The fit of the experimental data reveal a deformed octahedral geometry with the iron in the central position in the low-spin state. Temperature resolved EXAFS measurements indicate a reversible lengthening of the Fe–N distances in a temperature range up to 328 K. Magnetic properties of the films were investigated with SQUID magnetometer, spin resolved neutron reflectivity and X-ray magnetic circular dichroism (XMCD) [21,48]. The measurements revealed a magnetic moment of  $0.5 \mu_B/\text{Fe(II)}$  carried by the iron ions within the films above temperatures of 350 K. Fig. 6 shows the temperature dependent magnetic moment for two films consisting of 11 and 15 layers. Whereas the material behaves diamagnetic at low temperatures, an increasing paramagnetic signal above room temperature is observed. The curves for heating and cooling are indistinguishable indicating that there is no thermal hysteresis.

In thin LB films of PACs, melting of the alkyl chains in the amphiphilic mesophase causes distortion of the coordination geometry around the central transition metal ion. As a result, the effective crystal field splitting of the d-orbital subsets decreases resulting in a spin transition from a diamagnetic low-spin to a paramagnetic high-spin state.

## 4.2. Other examples of spin-crossover in thin films

An early example of spin-crossover in a Langmuir–Blodgett film is reported for amphiphilic Fe(II) complexes bearing semi-fluorinated chains [49,50]. The authors observed slightly less condensed packed alkyl chains compared to the bulk structure. As a consequence, the observed spin-crossover in the bulk is absent in the film until the alkyl chains melt. After melting the properties of the warmed LB films are similar to those of the complex in the bulk. The observed differences in magnetic behavior between films and bulk material are directly caused by the lamellar organization within LB multilayer.

Examples of thin films of spin-crossover compounds produced by alternative methods are reported for the layer-by-layer method [51] and spin-coating [52]. Referring the latter one, thin films of  $[\text{Fe}(\text{dpp})_2](\text{BF}_4)_2$  ( $\text{dpp} = 2,6\text{-di}(\text{pyrazol-1-yl})\text{pyridine}$ ) could be produced. The film shows a reversible spin-crossover of the Fe(II) ions at around  $T = 260\text{ K}$  [52]. This material is particularly interesting in the context of this article because it is based on 2,6-di(pyrazol-1-yl)pyridine ligands. With these ligands, similar supramolecular architectures could be achieved as they are found for tpy-based ligand systems (see also Section 6).

## 5. Volume material

### 5.1. Structural and magnetic properties of bulk PAC

The structure of bulk PAC was determined by a combination of molecular modelling and X-ray scattering [53]. Molecular modelling was used to compose and refine the PAC architecture until the calculated scattering curves match the experimental data [54]. Fig. 7 shows a representative model of the obtained PAC architecture.

The final PAC model shows a MEPE stratum between two close-packed amphiphile strata with interdigitated DHP molecules. Interestingly, this particular complex has six DHP molecules per metallo-polymer repeat unit, rather than the minimum of two needed for charge neutralization. The excess surfactants are asso-

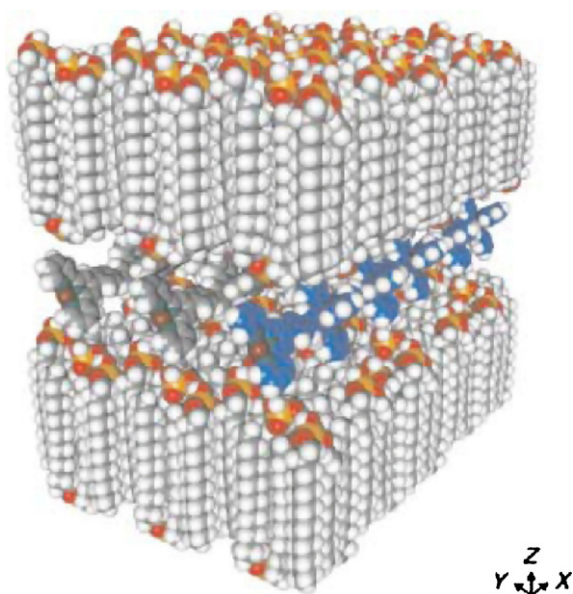


**Fig. 7.** PAC model showing two DHP strata and the interstitial MEPE layer derived from SAXS, WAXS and molecular modelling. Note the hierarchy of the architecture involving molecular, mesoscopic, and macroscopic length scales. Figure reproduced from Ref. [53].

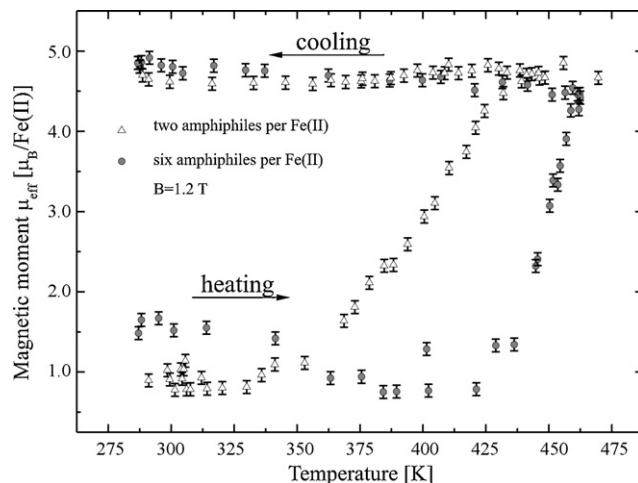


**Fig. 8.** Magnetic moment  $\mu_{\text{eff}}(T)$  of two PACs containing two (triangles) or six (circles) amphiphile molecules per Fe(II). The increase of the moment with temperature indicates a transition from diamagnetic low-spin state to a paramagnetic high-spin state of the Fe(II) ions. Both PAC show different spin-transition temperatures. The high-spin state persists upon cooling in all systems. Figure reproduced according Ref. [55].

ciated via hydrogen bonding (note that partially charged DHP contains both H-bond donor and acceptor sites). The number of DHP molecules per polymer repeat unit could be precisely adjusted by the assembly conditions. Solid-state structures of PAC confirmed by SAXS and WAXS measurements showed lamellar ordering with a repeat distance of  $33\text{ Å}$ , (Bragg position  $q \sim 0.2\text{ Å}^{-1}$ ) implying full interdigitation of DHP alkyl chains. By the use of energy-dispersive small angle X-ray scattering and magnetic measurements, a spin-crossover of the Fe(II) ions into a stable high-spin state above room temperature driven and stabilized by a structural phase transition is observed [55]. The temperature of spin-crossover scales with the number of amphiphilic molecules attached to the metallo-polymer backbone. In Fig. 8, the effective magnetic moment  $\mu_{\text{eff}}(T)$  measured by a Faraday-Balance for two PACs with a 1:2 and 1:6 ratio of metallo-polymer repeat unit to amphiphiles is shown. An increase of the magnetic moment indicates the spin-crossover. The low temperature magnetic behavior was proven with a SQUID magnetometer. While cooling, the magnetic moment decreases continuously. Fitting the data to the Curie-Weiss law reveals independently the same magnetic moment of  $\mu_{\text{eff}} \sim 4.8 \pm 0.2\text{ μ}_B/\text{Fe(II)}$  as found with the Faraday-Balance. These measurements confirm the persistence of the stable high-spin state of the Fe(II) ions down to low temperatures and we therefore rule out the presence of an uncompleted large thermal hysteresis as it is observed in other spin-crossover compounds [56,57]. The results further suggest a possible antiferromagnetic coupling between Fe(II) ions at very low temperatures as it was found for assemblies based on 4f metals and ditopic terpyridine ligands. The use of Yb(III) ions lead to antiferromagnetic coupling between the metal centers at  $\sim 13\text{ K}$  [58].

Temperature resolved energy-dispersive small angle X-ray scattering experiments revealed the high-spin state to be stabilized by a structural phase transition. Fig. 9 shows the collected SAXS pattern as function of temperature for the PAC with two amphiphiles per polymer repeat unit. The peak at  $q = 0.16\text{ Å}^{-1}$  is associated with the K-fluorescence of the Fe(II) ions. The two signals at  $q = 0.22\text{ Å}^{-1}$  and  $q = 0.44\text{ Å}^{-1}$  represent scattering peaks corresponding to the lamellar ordering mentioned above with a repeat distance of  $d = 29\text{ Å}$  for this particular PAC. At increasing temperature the two scattering peaks shift towards lower  $q$  reflecting the melting

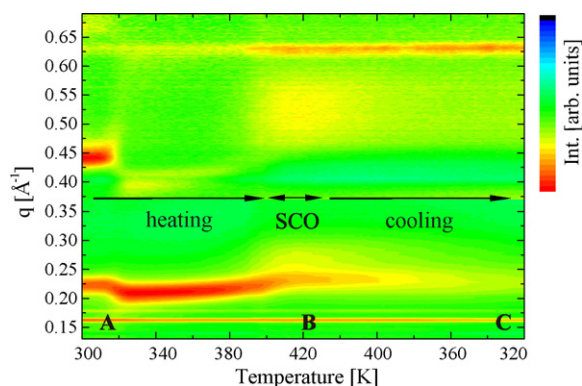


**Fig. 9.** Time resolved energy-dispersive SAXS pattern of PAC (time resolution of 60 s/spectrum). Between 300 and 330 K (position A) the peak shift indicates the melting of the amphiphilic phase. Above 400 K (position B) the peak broadens as a result of structural reorganization. Spin-crossover occurs in the temperature range indicated by SCO. Cooling to room temperature (position C) the SAXS pattern remains unchanged indicating a frozen state.

of the amphiphilic molecules. At the spin-crossover temperature observed with magnetic measurements, a new scattering peak appears characterizing a structural reorganization of the system. The resulting structure remains stable during cooling and stabilizes the high-spin state of the Fe(II) ions. The results suggest that the spin-crossover is induced and stabilized by the observed structural reorganization of the material.

In order to confirm our hypothesis that the spin transition is induced by the structural phase transition of the amphiphilic matrix, the PAC is prepared with  $\text{Ni}^{2+}$  as central ion. The Ni(II)-PAC is isostructural to the Fe(II)-PAC but is characterized by the absence of a spin transition. The magnetic moment of Ni(II)-PAC was measured for the same heating and cooling cycle described above. The observed magnetic moment of Ni(II)-PAC is estimated to be  $\mu_{\text{eff}} = 3.14 \mu_{\text{B}}/\text{Ni(II)}$  in agreement with literature values [59]. X-ray characterization reveals the same structural reorganization at

the same temperatures as found for the Fe(II)-PACs. The structural phase transition of the amphiphilic matrix embedding the metal center in PAC is not affected by the transition metal ion.

## 6. Rigid metallo-polymers and alternative ligand concepts

The PACs described so far are built by assembling metallo-supramolecular polymers (MEPEs) with amphiphilic molecules. These metallo-polymers based on ditopic terpyridine ligands possess a variety of attractive properties that make them interesting in photophysical, electrochemical, and magnetic studies [60]. In this section we want to address some basic properties of these metallo-polymers.

The solid-state structure of MEPE was recently solved using electron diffraction [61]. The data reveals a primitive monoclinic unit cell, in which the MEPE forms linear rods, which are organized into sheets. Mössbauer spectroscopy confirms the pseudo-octahedral coordination geometry around the Fe(II) ions and indicates an average length of approximately 8 repeat units in the solid state. As an example of a possible future application Co(II) based MEPEs can be incorporated as electrochromic active component in thin films [62].

A further method to modify the magnetic properties of metallo-polymers could be achieved by using triazine based ligands. Here, the central pyridine ring is replaced by triazine leading to a tpy-like ligand with reduced crystal field strength that can be complexed with different transition metal ions [63]. In this metallo-polymeric structure different spin states of the central Fe(II) ion could be obtained by different counter ions [64].

As already mentioned for thin films a structural alternative approach to spin-crossover complexes based on ditopic terpyridine ligands is the use of 2,6-di(pyrazol-1-yl)pyridine back-to-back ligands. Following this route spin-crossover behavior could be incorporated in rigid rod like metallo-polymers [24]. The linear iron(II) metallo-polymer (Fig. 10) shows a reversible spin transition at 323 K with a ca. 10 K wide hysteresis loop.

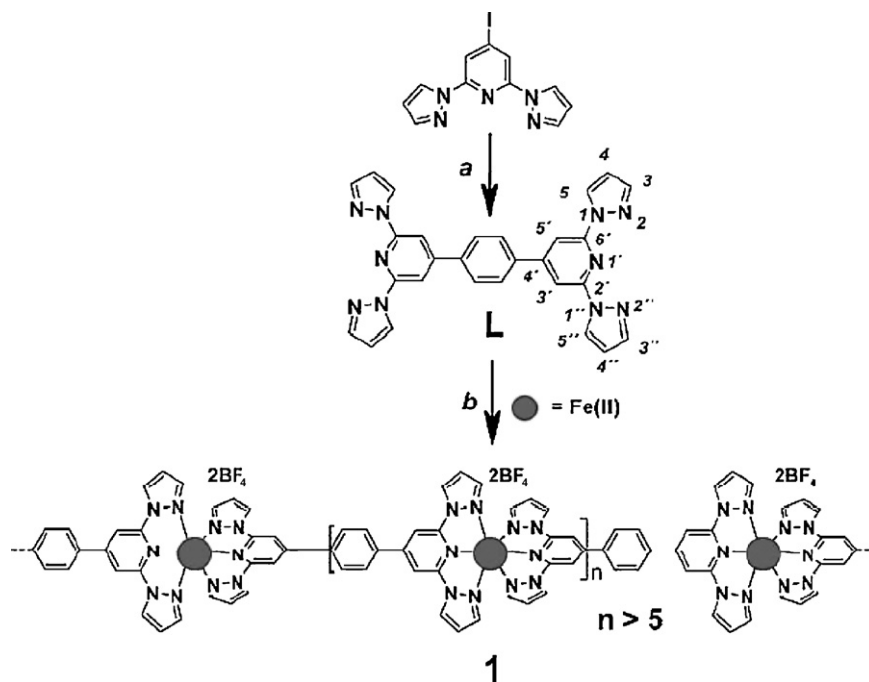


**Fig. 10.** The linear iron(II) coordination chain (1) based on 2,6-di(pyrazol-1-yl)pyridine ligands shows reversible spin transition at 323 K. Figure reproduced from Ref. [24].

## 7. Outlook and perspectives

The development of multifunctional spin-crossover materials reflects a modern trend in molecular materials science. There is hope that multifunctional SCO systems will find applications as sensors, molecular separators of gases, in photonic devices, light modulators and filters, rewritable molecular memory devices and image processing. To be useful in practice, a demanding set of material requirements must be met, such as room temperature operation, non-destructive writing and readout of the information. Nowadays, prototypes for functional materials where the spin-crossover is ligand-driven, induced thermally, by pressure or light have already been described. In order to extend the given strategies, structure-induced spin-crossover compounds have been introduced. In the frame of this article we have concentrated on PAC and their magneto-structural properties.

This article shows that the magnetic response of PACs can be controlled by the design of the supramolecular architecture at all length scales including constituents, composition, and self-assembly conditions. In LB films melting of the amphiphilic matrix causes a reversible but partial spin-crossover slightly above room temperature (320 K). In contrast, the bulk PAC undergoes a nearly complete spin-crossover with respect to the Fe(II) ions driven and stabilized by a major structural perturbation of the metallo-supramolecular coordination polyelectrolyte. The spin-crossover temperature (400 K) is higher than in the LB-film suggesting cooperative motion involving the amphiphilic matrix as well as the polymeric backbone, such as disassembly into discrete units with coordinatively unsaturated, high-spin metal centers. The high-spin state in the bulk material is permanent.

The differences in the magnetic response are attributed to the distinctive structure of thin films compared to bulk samples. Whereas in thin films the PACs are organized in preferentially oriented two-dimensional planes, the bulk phase is most likely composed of randomly oriented domains, which inhibit relaxation upon cooling.

The irreversible thermochromism, which is associated with the spin-crossover, could be employed as tag to indicate a temperature threshold e.g. in food safety. In the future it will be of interest to study how one can design the magnetic response function, including the temperature range of SCO and thermal hysteresis, through the choice of ligands, amphiphiles, metal ions stoichiometry and assembly conditions in these linear one-dimensional spin-crossover polymers.

## Acknowledgements

This work was supported by Deutsche Forschungsgemeinschaft as part of the priority program 1137 “Molecular Magnetism”. We thank V. Kataev and C. Golze for high-field ESR and SQUID measurements and H.-H. Klauss for Mößbauer spectroscopy. This work is partly based on experiments performed at the Swiss spallation neutron source SINQ, Paul Scherrer Institut, Villigen, Switzerland and on the BESSY II synchrotron Berlin, Germany.

## References

- [1] P. Güthlich, H.A. Goodwin (Eds.), *Spin Crossover in Transition Metal Compounds. Topics in Current Chemistry*, vols. 233–235, Springer, Berlin, 2004, p. 235.
- [2] O. Kahn, *Molecular Magnetism*, VCH, USA, 1993.
- [3] J.-M. Lehn, *Science* 295 (2002) 2400.
- [4] G.M. Whitesides, B. Grzybowski, *Science* 295 (2002) 2418.
- [5] G.J. Halder, C.J. Kepert, B. Moubarak, K.S. Murray, J.D. Cashion, *Science* 298 (2002) 1762.
- [6] J.-M. Lehn, *Proc. Natl. Acad. Sci.* 99 (2002) 4763.
- [7] O. Kahn, C.J. Martinez, *Science* 279 (1998) 44.
- [8] D. Gatteschi, A. Caneschi, L. Pardi, R. Sessoli, *Science* 265 (1994) 1054.
- [9] J.M. Manriquez, G.T. Yee, R.S. McLean, A.J. Epstein, J.S. Miller, *Science* 252 (1991) 1415.
- [10] S. Ferlay, T. Mallah, R. Ouahes, P. Veillet, M. Verdaguer, *Nature* 378 (1995) 701.
- [11] M. Kinoshita, P. Turek, M. Tamura, K. Nozawa, D. Shiomi, Y. Nakazawa, M. Ishikawa, M. Takahashi, K. Awaga, T. Inabe, Y. Maruyama, *Chem. Lett.* (1991) 1225.
- [12] R. Sessoli, D. Gatteschi, A. Caneschi, M.A. Novak, *Nature* 365 (1993) 141.
- [13] D. Gatteschi, R. Sessoli, *Angew. Chem. Int. Ed.* 42 (2003) 268.
- [14] A. Caneschi, D. Gatteschi, N. Lalioti, C. Sangregorio, R. Sessoli, G. Venturi, A. Vindigni, A. Rettori, M.G. Pini, M.A. Novak, *Angew. Chem. Int. Ed.* 40 (2001) 1760.
- [15] M. Balanda, M. Rams, S.K. Nayak, Z. Tomkiewicz, W. Haase, K. Tomala, J.V. Yakhmi, *Phys. Rev. B* 74 (2006) 224421.
- [16] C. Schröder, H.-J. Schmidt, J. Schnack, M. Luban, *Phys. Rev. Lett.* 94 (2005) 207203.
- [17] J.-M. Lehn, *Angew. Chem. Int. Ed.* 27 (1988) 89.
- [18] C.J. Pedersen, *Angew. Chem. Int. Ed.* 28 (1988) 1009.
- [19] D.J. Cram, *Angew. Chem. Int. Ed.* 27 (1988) 1021.
- [20] G.M. Whitesides, J.P. Mathias, C.T. Seto, *Science* 254 (1991) 1312.
- [21] Y. Bodenthin, U. Pietsch, H. Möhwald, D.G. Kurth, *J. Am. Chem. Soc.* 127 (2005) 3110.
- [22] Y. Bodenthin, U. Pietsch, J. Grenzer, Th. Geue, H. Möhwald, D.G. Kurth, *J. Phys. Chem. B* 109 (2005) 12795.
- [23] S. Hayami, Y. Shigeyoshi, M. Akita, K. Inoue, K. Kato, K. Osaka, M. Takata, R. Kawajiri, T. Mitani, Y. Maeda, *Angew. Chem. Int. Ed.* 44 (2005) 4899.
- [24] C. Rajadurai, O. Fuhr, R. Kruk, M. Ghafari, H. Hahn, M. Ruben, *Chem. Commun.* (2007) 2636.
- [25] M. Schadt, W. Helfrich, *Appl. Phys. Lett.* 18 (1971) 127.
- [26] Y. Galyametdinov, V. Ksenofontov, A. Prosvirin, I. Ovchinnikov, G. Ivanova, P. Güthlich, W. Haase, *Angew. Chem. Int. Ed.* 40 (2001) 4269.
- [27] M. Seredyuk, A.B. Gaspar, V. Ksenofontov, Y. Galyametdinov, J. Kusz, P. Güthlich, *J. Am. Chem. Soc.* 130 (2008) 1431.
- [28] S. Hayami, R. Moriyama, A. Shuto, Y. Maeda, K. Ohta, K. Inoue, *Inorg. Chem.* 46 (2007) 7692.
- [29] T. Fujigaya, D.-L. Jiang, T. Aida, *J. Am. Chem. Soc.* 125 (2003) 14690.
- [30] (a) G.S. Hanan, D. Volkmer, U.S. Schubert, J.M. Lehn, D. Fenske, *Angew. Chem.* 109 (1997) 1929 S;  
(b) C.S. Campos-Fernandez, R. Clerac, K.R. Dunbar, *Angew. Chem.* 111 (1999) 3685 S.
- [31] J. Rojo, J.-M. Lehn, G. Baum, D. Fenske, O. Waldmann, P. Müller, *Eur. J. Inorg. Chem.* 3 (1999) 517.
- [32] O. Waldmann, J. Hassmann, P. Müller, *Phys. Rev. Lett.* 78 (1997) 3390.
- [33] O. Waldmann, L. Zhao, L.K. Thompson, *Phys. Rev. Lett.* 88 (2002) 066401.
- [34] O. Waldmann, J. Hassmann, P. Müller, D. Volkmer, U.S. Schubert, J.-M. Lehn, *Phys. Rev. B* 58 (1998) 3277.
- [35] E. Breuning, M. Ruben, J.M. Lehn, F. Renz, Y. Garcia, V. Ksenofontov, P. Güthlich, E. Wegelius, K. Rissanen, *Angew. Chem.* 112 (2000) 2563;  
E. Breuning, M. Ruben, J.M. Lehn, F. Renz, Y. Garcia, V. Ksenofontov, P. Güthlich, E. Wegelius, K. Rissanen, *Angew. Chem. Int. Ed.* 39 (2000) 2504.
- [36] S. Decurtins, P. Güthlich, C.P. Köhler, H. Spiering, A. Hauser, *Chem. Phys. Lett.* 105 (1984) 1.
- [37] A. Desaix, O. Roubeau, J. Jeffit, J.G. Haasnoot, K. Boukheddaden, E. Codjovi, J. Linares, M. Nogues, F. Varret, *Eur. Phys. B* 6 (1998) 183.
- [38] E.C. Constable, M.D. Ward, *Inorg. Chim. Acta* 141 (1988) 201.
- [39] (a) E.C. Constable, A.M.W. Cargill Thompson, *J. Chem. Soc. Dalton Trans.* (1992) 2947;  
(b) E.C. Constable, D.R. Smith, *Supramol. Chem.* 4 (1994) 5.
- [40] E.C. Constable, J.E. Davies, D. Phillips, P.R. Raithby, *Polyhedron* 06 (1998) 3989.
- [41] E.C. Constable, G. Baum, E. Bill, R. Dyson, R. van Eldik, D. Fenske, S. Kaderli, D. Morris, A. Neubrand, M. Neuburger, D.R. Smith, K. Wieghardt, M. Zehnder, A.D. Zuberbühler, *Chem. Eur. J.* 5 (1999) 498.
- [42] M. Schütte, D.G. Kurth, M.R. Linfood, H. Cölfen, H. Möhwald, *Angew. Chem. Int. Ed.* 37 (1998) 2891.
- [43] E.C. Constable, *Chem. Soc. Rev.* 36 (2007) 246.
- [44] D.G. Kurth, P. Lehmann, M. Schütte, *Proc. Natl. Acad. Sci.* 97 (2000) 5704.
- [45] Y. Bodenthin, J. Grenzer, R. Lauter, U. Pietsch, P. Lehmann, D.G. Kurth, H. Möhwald, *J. Synchrotron Radiat.* 9 (2002) 206.
- [46] P. Lehmann, D.G. Kurth, G. Brezesinski, Ch. Symietz, *Chem. Eur. J.* 7 (2001) 1646.
- [47] U. Pietsch, T.A. Barberka, U. Englisch, R. Stömmmer, *Thin Solid Films* (1996) 284, 387.
- [48] Y. Bodenthin, G. Schwarz, Th. Gutberlet, Th. Geue, J. Stahn, H. Möhwald, D.G. Kurth, U. Pietsch, *Superlatt. Microstruct.* 41 (2007) 138.
- [49] H. Soyer, E. Dupart, C.J. Gomez-Garcia, C. Mingotaud, P. Delhaes, *Adv. Mater.* 11 (1999) 382.
- [50] H. Soyer, E. Dupart, C. Mingotaud, C.J. Gomez-Garcia, P. Delhaes, *Colloids Surf. A* 171 (2000) 275.
- [51] S. Cobo, G. Molnar, J.A. Real, A. Bousseksou, *Angew. Chem. Int. Ed.* 45 (2006) 5786.
- [52] M. Matsuda, H. Tajima, *Chem. Lett.* 36 (2007) 700.
- [53] A. Meister, G. Förster, A.F. Thünemann, D.G. Kurth, *ChemPhysChem* 4 (2003) 1095.
- [54] D.G. Kurth, A. Meister, A.F. Thünemann, G. Förster, *Langmuir* 19 (2003) 4055.



- [55] Y. Bodenthin, G. Schwarz, Z. Tomkowicz, A. Nefedov, M. Lommel, H. Möhwald, W. Haase, D.G. Kurth, U. Pietsch, *Phys. Rev. B* 76 (2007) 064422.
- [56] J.-F. Letard, J.A. Real, N. Moliner, A.B. Gaspar, L. Capes, O. Cadot, O. Kahn, *J. Am. Chem. Soc.* 121 (1999) 10630.
- [57] S. Hayami, T. Kawahara, G. Juhasz, K. Kawamura, K. Uehashi, O. Sato, Y. Maeda, *J. Radioanal. Nucl. Chem.* 255 (2003) 443.
- [58] C.N. Carlson, C.J. Kuehl, R.E. Da Re, J.M. Veauthier, E.J. Schelter, A.E. Milligan, B.L. Scott, E.D. Bauer, J.D. Thompson, D.E. Morris, K.D. John, *J. Am. Chem. Soc.* 128 (2006) 7230.
- [59] O. Waldmann, J. Hassmann, P. Müller, D. Volkmer, U.S. Schubert, J.M. Lehn, *Phys. Rev. B* 58 (1998) 3277.
- [60] D.G. Kurth, M. Higuchi, *Soft Matter* 2 (2006) 1.
- [61] U. Kolb, K. Bücher, C.A. Helm, A. Lindner, A.F. Thünemann, M. Menzel, M. Higuchi, D.G. Kurth, *Proc. Natl. Acad. Sci. U.S.A.* 103 (2006) 10202.
- [62] D.G. Kurth, J.P. Lopez, W.F. Dong, *Chem. Commun.* (2005) 2119.
- [63] E.A. Medlycott, K.A. Udachin, G.S. Hanan, *Dalton Trans.* (2007) 430.
- [64] E.A. Medlycott, G.S. Hanan, T.S.M. Abedin, L.K. Thompson, *Polyhedron* 27 (2008) 493.